

Decision-Oriented Learning with Differentiable Submodular Maximization for Vehicle Routing Problem

Guangyao Shi, Pratap Tokekar

Abstract—We study the problem of learning a function that maps context observations (input) to parameters of a submodular function (output). Our motivating case study is a specific type of vehicle routing problem, in which a team of Unmanned Ground Vehicles (UGVs) can serve as mobile charging stations to recharge a team of Unmanned Ground Vehicles (UAVs) that execute persistent monitoring tasks. We want to learn the mapping from observations of UAV task routes and wind field to the parameters of a submodular objective function, which describes the distribution of landing positions of the UAVs. Traditionally, such a learning problem is solved independently as a prediction phase without considering the downstream task optimization phase. However, the loss function used in prediction may be misaligned with our final goal, i.e., a good routing decision. Good performance in the isolated prediction phase does not necessarily lead to good decisions in the downstream routing task. In this paper, we propose a framework that incorporates task optimization as a differentiable layer in the prediction phase. Our framework allows end-to-end training of the prediction model without using engineered intermediate loss that is targeted only at the prediction performance. In the proposed framework, task optimization (submodular maximization) is made differentiable by introducing stochastic perturbations into deterministic algorithms (i.e., stochastic smoothing). We demonstrate the efficacy of the proposed framework using synthetic data. Experimental results of the mobile charging station routing problem show that the proposed framework can result in better routing decisions, e.g. the average number of UAVs recharged increases, compared to the prediction-optimization separate approach.

I. INTRODUCTION

Multi-robot teams are widely used in information gathering, environment monitoring, exploration, and target tracking [1]–[3]. Many multi-robot decision-making problems can be formulated as combinatorial optimization problems [4], among which the objectives in some problems (e.g., mutual information [5], area explored, number of targets tracked [6], detection probability [7] etc.) have diminishing returns property i.e., submodularity. Intuitively, submodularity formalizes the notion that adding more robots to a larger multi-robot team cannot yield a larger marginal gain in the objective than adding the same robot to a smaller team. We are interested in considering maximizing such submodular objectives.

If the submodular objective is known and fixed, the multi-robot decision-making problem boils down to a submodular maximization problem, which is NP-hard but can be solved with an $(1 - \frac{1}{e})$ -approximation by the greedy algorithm [8]. However, in practice, there are a number of parameters that

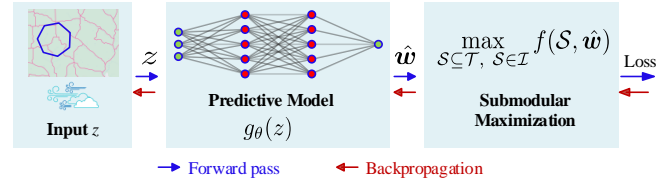


Fig. 1. In Decision-Oriented Learning, we train the predictive model using the loss from the downstream task. The key requirement here is to make the submodular maximization differentiable for the loss to be backpropagated to the predictive model.

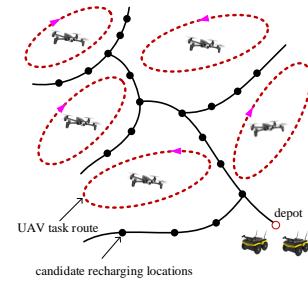


Fig. 2. An illustrative example for mobile charging station routing problems.

affect the objective function that may not be known exactly.

Consider the following illustrative example of a vehicle routing problem shown in Figure 2. Here, a team of Unmanned Ground Vehicles (UGVs) are tasked with servicing a set of requests that appear throughout the environment. We have a set of candidate routes of which we must select one for each UGV. The objective is to maximize the number of requests serviced. If a request location lies on more than one UGVs path (the paths may overlap as the UGVs move on a road network), it only counts once in the objective function. Thus, the objective function is a coverage function, which is a special case of the submodular function.

If we know the location of the requests, then we can solve this problem greedily to obtain a $(1 - \frac{1}{e})$ -approximation. The greedy algorithm requires the capability to compute the objective function $f(S)$. However, there are many scenarios where we may not know where the requests show up and as such not know $f(S)$. For example, the requests could correspond to Unmanned Aerial Vehicles (UAVs) that are carrying out persistent monitoring missions that land when out of charge so as to be recharged by mobile recharging stations [9]–[14]. Here, even if we know the routes followed by each UAV, we may not know their exact landing locations

This work is supported in part by National Science Foundation Grant No. 1943368 and Army Grant No. W911NF2120076.

Guangyao Shi, Pratap Tokekar are with the University of Maryland, College Park, MD 20742 USA [gyshi, tokekar]@umd.edu

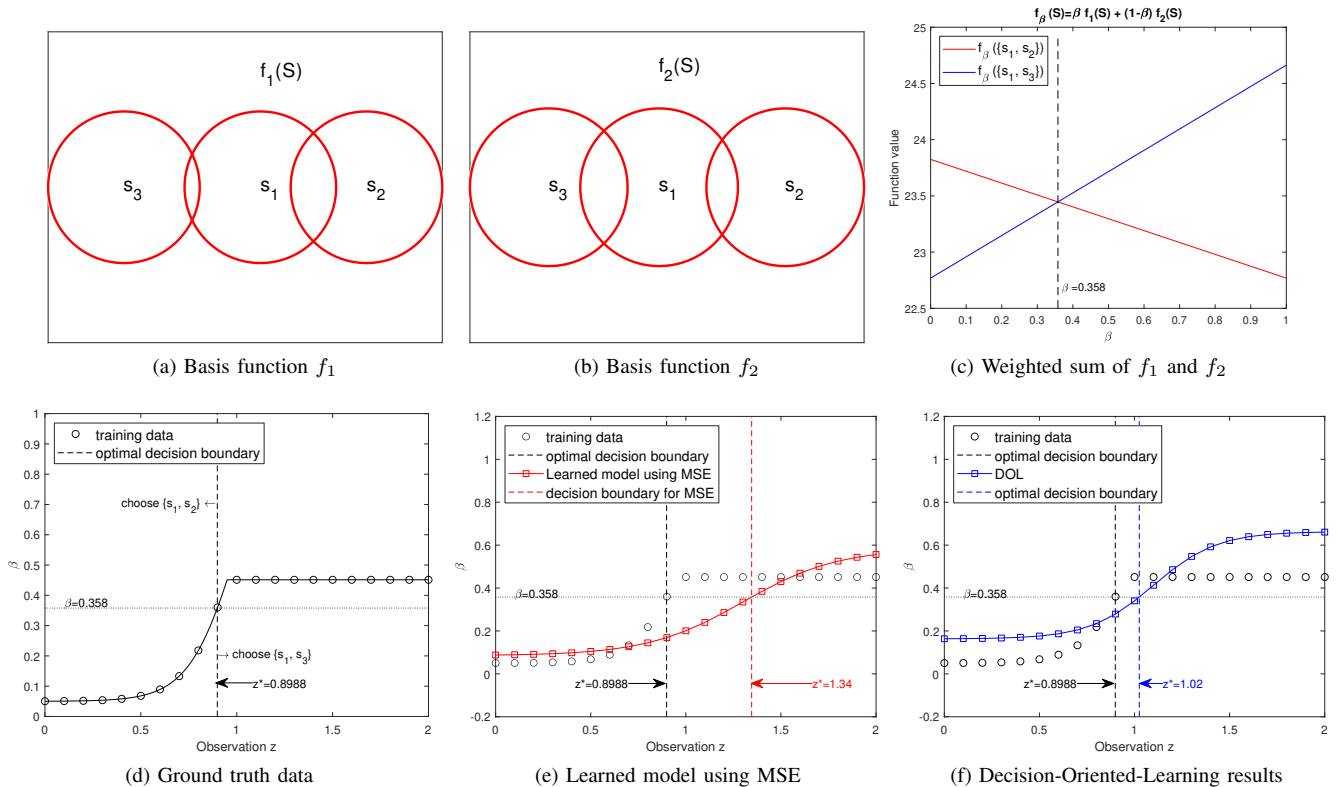


Fig. 3. An illustrative example to show the misalignment between the prediction model that achieves high predictive accuracy and the one that results in good decisions.

since the energy consumption is stochastic [13], [14] and communication between UAVs and UGVs is not available (e.g., due to stealth). In such cases, we may be able to predict $f(S)$ using all the available information. We call the latter as *context* z . The context can include the routes of the UAVs, the environmental conditions including the wind conditions, etc.

The traditional pipeline here would be to use the context information and predict $f(S)$ and then solve the downstream UGV route selection problem, $\operatorname{argmax}_S \hat{f}(S)$, using this predicted $\hat{f}(S)$. However, as the following example shows a good predictor of $f(S)$ does not necessarily align with making good decisions on the downstream task. On the other hand, a predictor that does not necessarily yield the best predictions of $f(S)$ may still yield the best decisions for the downstream $\operatorname{argmax}_S \hat{f}(S)$ problem.

We present an illustrative example of such misalignment in Fig. 3. Let f_1, f_2 be two coverage functions (coverage function is submodular by definition) defined over set $\{s_1, s_2, s_3\}$. Given a subset $S \subseteq \{s_1, s_2, s_3\}$, $f_i(S), i = 1, 2$ will return the area covered by the selection. The submodular objective that we are interested in is defined as $f_\beta(S) = \beta f_1(S) + (1 - \beta) f_2(S), \beta \in [0, 1]$, which is also submodular by definition. Suppose that we want to maximize f_β with a partition matroid: $|\mathcal{S} \cap \{s_1\}| \leq 1, |\mathcal{S} \cap \{s_2, s_3\}| \leq 1$. Then the optimal solution is either $\{s_1, s_2\}$ or $\{s_1, s_3\}$. In Fig. 3c, we show how the optimal decision changes w.r.t. β . When $\beta \geq 0.358$, the optimal decision is $\{s_1, s_3\}$ since

$f_\beta(\{s_1, s_3\}) \geq f_\beta(\{s_1, s_2\})$ (the blue line is above the red line). By contrast, when $\beta < 0.358$, the optimal decision is $\{s_1, s_2\}$. Next, let us look at the learning problem for f_β . We want to find a mapping from the observation z to β . In Fig. 3d, we show the training data sampled from the ground truth and the optimal decision boundary $z^* = 0.8988$, which is obtained by finding the intersection between the ground truth curve and $\beta = 0.358$. If we use Mean Square Error (MSE) as the objective for learning without considering the downstream task, we will get two lines as shown in Fig. 3e. The decision boundary (dashed vertical red line, $z^* = 1.34$, passing the intersection of the learned red line and $\beta = 0.358$) is on the right of the optimal boundary, thus not optimal. By contrast, if we consider the downstream optimization, we will get two lines as shown in Fig. 3f and the decision boundary (dashed vertical blue line, $z^* = 1.02$, passing the intersection of the learned blue line and $\beta = 0.358$) is closer to the optimal boundary, thus reducing the regions of suboptimal decisions. Such an observation motivates us to incorporate the decision process (submodular maximization) into the learning process and achieve end-to-end training.

To this end, we propose a Decision-Oriented-Learning (DOL) framework for learning context-aware parameterized submodular objectives. We focus on submodular functions that can be parameterized, i.e., $f(S, w)$, where the parameters are to be learned from the context (details on how to obtain training data will be explained in Sec. VI). As

described earlier and pointed out in [15]–[17], the best estimator of w does not necessarily yield the best decisions for the downstream task. Instead, in the proposed framework, the decision-making problem (submodular maximization) is treated as a differentiable layer which takes as input the output from the prediction module as shown in Fig. 1. The prediction module takes as input a context observation z and predicts w , i.e., the parameterized submodular function. By using a differentiable submodular optimization layer, we can train the prediction module using the loss from the downstream task, thereby yielding aligned predictions.

In summary, the main contribution is this paper is:

- We propose a decision-oriented learning framework for mobile charging routing problems. We show how to formulate the learning problem for mobile charging routing and how to make submodular maximization a differentiable layer by using stochastic smoothing techniques.
- We demonstrate the effectiveness of our framework in several examples through simulation.

The rest of the paper is organized as follows. We first give a brief overview of the related work in Section II. Then, we explain the problem setup and formulation in Section III. We introduce the learning algorithm in Section V and validate the formulation and the proposed framework in Section VI.

II. RELATED WORK

Most existing multi-robot decision-making work consider the case where the optimization objective is well-defined and known. Wilde et al. [18] study the environment monitoring problem from a different perspective in recent work. They consider the case where the optimization objective is hard to quantitatively specify and may be subjective and proposed an interactive learning framework to learn the objectives. Our work shares a similar stance with [18] but differs in two aspects. First, we consider the fact that the task objective may change in different contexts, for example in different weather conditions, and aim at learning a context-aware objective. Second, our learning framework integrates the downstream decision-making process into the learning process.

Another line of research related to this work is decision-oriented learning. The key idea is to embed the decision-making problem as a differentiable layer in the learning pipelines. The main advantage is that it allows end-to-end training and reduces the engineering efforts to design some intermediate learning objectives. Such an idea was initially explored for continuous optimization problems [19], [20] and has gained popularity in control and robotics [21]–[24]. The idea was later extended to the combinatorial problems [16], [17], [25], [26]. Our work is inspired by [16], [25] and our framework integrates the decision-making process for mobile charging station routing, which is modeled as submodular maximization, into the learning process.

This work is also closely related to differentiable submodular maximization. Submodular maximization and its variants have been widely used in multi-robot decision-making problems including coverage, target tracking, ex-

ploration, and information gathering. These studies are all based on the fact that the greedy algorithm and its variants can solve submodular maximization problems its variants efficiently with a provable performance guarantee. Since the submodular objective and greedy algorithm are tightly coupled, it is better to take into account the influence of the greedy algorithm when we consider learning submodular functions [27]. To this end, several differentiable versions of the greedy algorithms have been proposed [27], [28]. The core idea behind these algorithms is stochastic smoothing, i.e., perturb the algorithm by introducing some probability distribution in the intermediate steps. Our framework is built on these differentiable greedy algorithms but is targeted specifically for context-dependent routing problems.

III. PROBLEM FORMULATION

In this section, we first introduce the formulation of the learning problem. Then, we explain the setup of the case study and the parameterization of the objective.

Definition 1 (Submodularity). For a set \mathcal{V} , a function $f : 2^{\mathcal{V}} \mapsto \mathbb{R}$ is submodular if and only if for any sets $\mathcal{A} \subseteq \mathcal{V}$ and $\mathcal{A}' \subseteq \mathcal{V}$, we have $f(\mathcal{A}) + f(\mathcal{A}') \geq f(\mathcal{A} \cup \mathcal{A}') + f(\mathcal{A} \cap \mathcal{A}')$.

We are interested in parameterized submodular objective function $f(\mathcal{S}, w)$, where w is the parameter vector. In practice, such an objective is usually unknown and context-dependent, i.e., the parameters $w \in \mathcal{W}$ depend on the environment features. Our goal is to learn a function $g_{\theta} : \mathcal{Z} \rightarrow \mathcal{W}$ that maps the context observation $z \in \mathcal{Z}$ to the objective parameters w . Traditionally, finding the mapping g_{θ} and optimizing the downstream objective $f(\mathcal{S}, w)$ are considered separately: given the training data $\mathcal{D} = \{(z_1, w_1), (z_2, w_2), \dots, (z_{|\mathcal{D}|}, w_{|\mathcal{D}|})\}$, first find the mapping g_{θ} by optimizing over θ in a supervised fashion, and then use the parameter $w = g_{\theta}(z)$ to optimize $f(\mathcal{S}, w)$.

By contrast, a paradigm that integrates downstream optimization into the parameter estimation process is attracting increasing attention. We are interested in using such a new paradigm to find the mapping from the environment context features to the objective parameters. The formal statement of our problem is given below.

Problem 1. Given the training data $\mathcal{D} = \{(z_1, w_1), (z_2, w_2), \dots, (z_{|\mathcal{D}|}, w_{|\mathcal{D}|})\}$, learn a function g_{θ} parameterized by θ such that the learning cost $L = \frac{1}{|\mathcal{D}|} \sum_{i=1}^{|\mathcal{D}|} \ell_i(w_i, \hat{w}_i)$ is minimized, where $\ell_i(w_i, \hat{w}_i)$ is defined through Eq. (1) to Eq. (3):

$$\hat{w}_i := g_{\theta}(z_i) \quad (1)$$

$$\hat{\mathcal{S}} := \mathcal{S}^*(\hat{w}_i) \text{ by solving (5) with } w = \hat{w}_i \quad (2)$$

$$\ell_i(\hat{w}_i, w_i) := f(\mathcal{S}^*(w_i), w_i) - f(\hat{\mathcal{S}}, w_i), \quad (3)$$

where $\mathcal{S}^*(w_i)$ denotes the solution of (5) returned by some approximation algorithms with $w = w_i$; $f(\mathcal{S}^*(w_i), w_i)$ denotes the decision quality when we use the ground truth parameter w_i for decisions; $f(\hat{\mathcal{S}}, w_i)$ denotes the decision

quality when we use the predicted parameter \hat{w}_i for decisions, i.e., use \hat{w}_i to obtain the decision \mathcal{S} , but the decision is evaluated w.r.t. the true parameter w_i .

The intuition for Eq. (3) is that we want to minimize the gap between the decision quality of the true parameters and that of the predicted parameters. One challenge is when we use the chain rule to compute the gradient of the loss function, we need to differentiate through the optimization problem (the first term on the r.h.s. of Eq. (4)) as shown in the illustrative computational graph in Fig. 1.

$$\frac{\partial \ell_i}{\partial \theta} = \frac{\partial \ell_i}{\partial \hat{w}_i} \cdot \frac{\partial \hat{w}_i}{\partial \theta} \quad (4)$$

In the following sections, we will show how to approximately compute the first term on the r.h.s. of Eq. (4).

IV. CASE STUDY: MOBILE CHARGING STATION ROUTING

Suppose that there is a set of candidate routes, \mathcal{T} , each of which starts and terminates at the same depot. Our goal is to select a subset from \mathcal{T} for UGVs to traverse and recharge the UAV along the way such that the total number of UAVs that UGVs will recharge is maximized.

Environment Model: As shown in Fig. 2, the working environment is described by an area $\mathcal{E} \subseteq \mathbb{R}^2$. There are n_a UAVs that are executing persistent monitoring. The energy consumption of UAVs will be affected by the wind. The wind field is represented as a tuple (ω_s, ω_o) , where ω_s and ω_o denote the description vectors for the speed and the orientation of the wind, respectively. Wind speed is a random variable with Weibull distribution. There are n_g UGVs in \mathcal{E} , denoted by the set $\{1, \dots, n_g\}$. The UGVs are constrained to the road $\bar{\mathcal{E}} \subset \mathcal{E}$. We consider the case that the road is discretized and represented as a graph $G = (V, E)$.

UAV Behavior: There are three components defining the behavior of each UAV. The first one is the task route, which is defined as a sequence of ordered locations projected on the ground, and the UAV will persistently monitor these locations. The UAV will fly at a fixed speed v_a between two task locations and its energy consumption will be affected by the wind. The second component is the recharging strategy dealing with the depletion of the battery. The third component is the energy consumption model. We use the same model as that in [29]. Specifically, when the UAV traverses one edge in its task route, the energy consumption is a function of the length of the edge, the relative flight direction w.r.t. the wind direction, the speed of the UAV, and the speed of the wind. More details can be found in Appendix.

Context Observation: Each observation z consists of two components: the task routes of all UAVs; and the wind field (ω_s, ω_o) of the working area.

If such submodular objective f is known, the problem boils down to a submodular maximization problem with a matroid constraint: let \mathcal{T} be set of all candidate routes, the problem is to select a subset from \mathcal{T} to maximize the

objective, i.e.,

$$\max_{\mathcal{S} \subseteq \mathcal{T}, |\mathcal{S}| \leq n_g} f(\mathcal{S}, \mathbf{w}), \quad (5)$$

where \mathbf{w} denotes the parameters in the objective function.

Parameterization of the Objective Function In general, there is no closed-form expression of the objective function in such applications. In this paper, we consider the case where the objective function f is the linear combinations of a set of basis functions $f_1, \dots, f_n : 2^{\mathcal{T}} \rightarrow \mathbb{R}_{\geq 0}$. Such parameterization techniques are commonly used in the literature on learning submodular functions [7], [18], [30]. Given the route selection \mathcal{S} , $f(\mathcal{S}, \mathbf{w})$ can be computed as $f(\mathcal{S}, \mathbf{w}) = \sum_{i=1}^n w_i f_i(\mathcal{S})$, where w_i is a context-dependent weight.

Similar to [18], we assume without loss of generality that each basis function is characterized by a subset $W_i \subseteq V$. That is, for any W_i , let $\psi_i(\mathcal{S})$ be a count of how many vertices of the tours \mathcal{S} lie in W_i , then f_i is a functional of $\psi_i(\mathcal{S})$.

The subsets W_1, \dots, W_n can be generated by dividing the graph G based on geometry or can be grouped according to the properties of the nodes in G . To account for the submodularity property of the objective [18], we choose the basis function to be

$$f_{i,j}(\mathcal{S}) = \sum_{\alpha=1}^{\psi_i(\mathcal{S})} \gamma_j^{(\alpha-1)}, \quad (6)$$

where γ_j comes from a known set Γ and $\gamma_j \in (0, 1]$. If $\gamma_j = 1$, $r_{i,j}(\mathcal{S})$ is equal to $\psi_i(\mathcal{S})$, i.e., the count of how many vertices in W_i ; by contrast, if $\gamma_j \rightarrow 0$, we do not obtain more rewards by visiting more than one vertex in W_i .

Using these basis functions, the overall objective function becomes

$$f(\mathcal{S}, \mathbf{w}) = \sum_{i=1}^n \sum_{j=1}^{|\Gamma|} w_{i,j} f_{i,j}(\mathcal{S}), \quad (7)$$

where $\mathbf{w} = [w_{i,j}]$ denotes the matrix of unknown parameters of the function. As shown in [18], the objective function $f(\mathcal{S}, \mathbf{w})$ proposed in Eq. (7) is a normalized, monotone, and submodular set function.

V. LEARNING ALGORITHM

In this section, we describe the stochastic techniques to smoothe the greedy algorithm for submodular maximization and how can we apply the result to our framework. The key idea is: the output of a combinatorial optimization as a function of its parameters may be discontinuous and non-differentiable. By introducing proper stochastic perturbances into the problem, the expected output as a function of its parameters can be smoothed and differentiable.

In the following, we will first introduce a smoothed version of the classic greedy algorithm. Then, we will show how to estimate the output gradient w.r.t. the objective parameters and explain how can we use this result in our framework.

Algorithm 1: Smoothed Greedy

Input :

- A submodular function $f(\mathcal{S}, \mathbf{w})$ parameterized by \mathbf{w}
- Independent set \mathcal{I}

Output: Set \mathcal{S} of tours for each robot

```
1  $\mathcal{S} \leftarrow \emptyset$ 
2 for  $k \leftarrow 1$  to  $N$  do
  // find all addable elements in the current round
3   $U_k = \{u_1, u_2, \dots, u_{n_k}\} \leftarrow \{T \notin \mathcal{S} \mid \mathcal{S} \cup \{T\} \in \mathcal{I}\}$ 
  // compute the marginal gain for all addable elements
4   $\mathbf{m}_k(\mathbf{w}) \leftarrow (f_{\mathcal{S}}(u_1, \mathbf{w}), \dots, f_{\mathcal{S}}(u_{n_k}, \mathbf{w}))$ 
  // compute a probability distribution over add elements
5   $\mathbf{p}_k(\mathbf{w}) \leftarrow \operatorname{argmax}_{\mathbf{p} \in \Delta^{n_k}} \{\langle \mathbf{m}_k(\mathbf{w}), \mathbf{p} \rangle - \Omega_k(\mathbf{p})\}$ 
  // sample one element
6   $s_k \leftarrow u \in U_k$  with probability  $p_k(u, \mathbf{w})$ 
  // update  $\mathcal{S}$ 
7   $\mathcal{S} \leftarrow \mathcal{S} \cup \{s_k\}$ 
8 end
9 return  $\mathcal{S}$ 
```

A. Smoothed Greedy Algorithm

The Smoothed Greedy (SG) algorithm is given in Algorithm 1, which was first proposed in [28]. For a given $\mathbf{w} \in \mathcal{W}$, In each iteration step, we compute marginal gain $f_{\mathcal{S}}(u, \mathbf{w})$ for each candidate element $u \in U_k$ (line 3); we define $n_k := |U_k|$. Let $\mathbf{m}_k(\mathbf{w}) = (m_k(u_1, \mathbf{w}), m_k(u_2, \mathbf{w}), \dots, m_k(u_{n_k}, \mathbf{w})) \in \mathbb{R}^{n_k}$ denote the marginal gain vector. The probability vector, $\mathbf{p}_k(\mathbf{w}) = (p_k(u_1, \mathbf{w}), \dots, p_k(u_{n_k}, \mathbf{w}))$, is computed as

$$\mathbf{p}_k(\mathbf{w}) = \operatorname{argmax}_{\mathbf{p} \in \Delta^{n_k}} \{\langle \mathbf{m}_k(\mathbf{w}), \mathbf{p} \rangle - \Omega_k(\mathbf{p})\}, \quad (8)$$

where $\Delta^{n_k} := \{\mathbf{p} \in \mathbb{R}^{n_k} \mid \mathbf{p} \geq \mathbf{0}_{n_k}, \langle \mathbf{p}, \mathbf{1}_{n_k} \rangle = 1\}$ is the $(n_k - 1)$ -dimensional probability simplex; $\Omega_k : \mathbb{R}^{n_k} \rightarrow \mathbb{R}$ is a strictly convex function and is a regularization function.

Next, we will show the theoretical results for Algorithm 1. Detailed explanations and proofs can be found in [28]. Let $\delta \geq 0$ be a constant that satisfies $\delta \geq \Omega_k(\mathbf{p}) - \Omega_k(\mathbf{q})$ for all $k = 1, \dots, |\mathcal{S}|$ and $\mathbf{p}, \mathbf{q} \in \Delta^{n_k}$. We will use δ to quantify the performance of SG.

As shown in Theorem 1 in [28], in expectation, the output of SG satisfies that

$$\mathbb{E}[f(\mathcal{S}, \mathbf{w})] \geq (1 - \frac{1}{e})f(OPT, \mathbf{w}) - \delta n_g,$$

where OPT denotes the optimal solution. This result suggests that the SG algorithm in expectation almost preserves the performance of the deterministic greedy algorithm, whose approximation factor is $(1 - \frac{1}{e})$, with one extra term δn_g , which is the price for differentiability. It should be noted that by using SG, the output is stochastic and we focus on the expected result of the output.

The regularization functions Ω_k are chosen to guarantee the expected outputs of SG differentiable. Examples for Ω_k will be discussed in the Sec. VI.

B. Gradient Estimation

Let $\mathcal{O}_{\mathcal{I}}$ be the set of all possible solutions returned by SG. Let $p(\mathcal{S}, \mathbf{w}) \in [0, 1]$ denote the probability for $\mathcal{S} \in \mathcal{O}_{\mathcal{I}}$. Specifically, for a returned sequence $\mathcal{S} = \{s_1, \dots, s_{|\mathcal{S}|}\} \in \mathcal{O}_{\mathcal{I}}$, the associated probability can be computed as

$$p(\mathcal{S}, \mathbf{w}) = \prod_{k=1}^{|\mathcal{S}|} p_k(s_k, \mathbf{w}), \quad (9)$$

where $p_k(s_k, \mathbf{w})$ is the element of $\mathbf{p}_k(\mathbf{w})$ defined Eq. (8) corresponding to $s_k \in U_k$.

Next, we will show how to construct a gradient estimator based on the output distribution. Let $Q(\mathcal{S})$ be any scalar- or vector-valued function. We want to compute $\nabla_{\mathbf{w}} \mathbb{E}_{\mathcal{S} \sim p(\mathbf{w})} [Q(\mathcal{S})] = \sum_{\mathcal{S} \in \mathcal{O}_{\mathcal{I}}} Q(\mathcal{S}) \nabla_{\mathbf{w}} p(\mathcal{S}, \mathbf{w})$. Since the size of the independent set will increase exponentially w.r.t. the size of the ground set, it is computationally expensive to compute this gradient exactly. Instead, we will use the following unbiased estimator for the gradient in training.

As shown in Proposition 1 in [28], let $\mathcal{S}_j = (s_1, \dots, s_{|\mathcal{S}_j|}) \sim p(\mathbf{w})$ ($j = 1, \dots, N$) be outputs of SG. Then

$$\frac{1}{N} \sum_{j=1}^N Q(\mathcal{S}_j) \otimes \nabla_{\mathbf{w}} \ln p(\mathcal{S}_j, \mathbf{w}) \quad (10)$$

is an unbiased estimator of $\nabla_{\mathbf{w}} \mathbb{E}_{\mathcal{S} \sim p(\mathbf{w})} [Q(\mathcal{S})]$, where \otimes denotes the outer product.

Next, we will show how to use this estimator for decision-oriented learning.

C. Differentiable Submodular Maximization for DOL

For the i -th training sample (z_i, \mathbf{w}_i) , the associated cost w.r.t. $\boldsymbol{\theta}$ is redefined for SG as¹

$$\ell_i(\hat{\mathbf{w}}_i, \mathbf{w}_i) := f(\mathcal{S}^*(\mathbf{w}_i), \mathbf{w}_i) - \mathbb{E}_{\hat{\mathcal{S}} \sim p(\hat{\mathbf{w}}_i)} [f(\hat{\mathcal{S}}, \mathbf{w}_i)], \quad (11)$$

where $\hat{\mathbf{w}}_i = g(z_i, \boldsymbol{\theta})$.

For a training set with batch size M , we are interested in minimizing the empirical objective function $\frac{1}{M} \sum_{i=1}^M \ell_i$, where $p(\hat{\mathbf{w}})$ is the output distribution of SG and ℓ_i is defined in Eq. (11).

We compute the gradient using the chain rule

$$\frac{\partial \ell_i}{\partial \boldsymbol{\theta}} = \frac{\partial \ell_i}{\partial \hat{\mathbf{w}}_i} \cdot \frac{\partial \hat{\mathbf{w}}_i}{\partial \boldsymbol{\theta}} = - \frac{\partial \mathbb{E}_{\hat{\mathcal{S}} \sim p(\hat{\mathbf{w}}_i)} [f(\hat{\mathcal{S}}, \mathbf{w}_i)]}{\partial \hat{\mathbf{w}}_i} \cdot \frac{\partial \hat{\mathbf{w}}_i}{\partial \boldsymbol{\theta}}, \quad (12)$$

where $\hat{\mathbf{w}} = g(z_i, \boldsymbol{\theta})$.

Suppose we take N trials of SG, by setting $Q(\hat{\mathcal{S}}) = f(\hat{\mathcal{S}}, \mathbf{w}_i)$ in Eq. (10), we have

$$\begin{aligned} & \text{r.h.s. of (12)} \\ &= \frac{-1}{N} \sum_{j=1}^N f(\hat{\mathcal{S}}_j, \mathbf{w}_i) \otimes \nabla_{\hat{\mathbf{w}}_i} \ln p(\hat{\mathcal{S}}_j, \hat{\mathbf{w}}_i) \cdot \frac{\partial \hat{\mathbf{w}}_i}{\partial \boldsymbol{\theta}}, \end{aligned} \quad (13)$$

¹We replace the deterministic term in Eq. (3) with one expectation term.

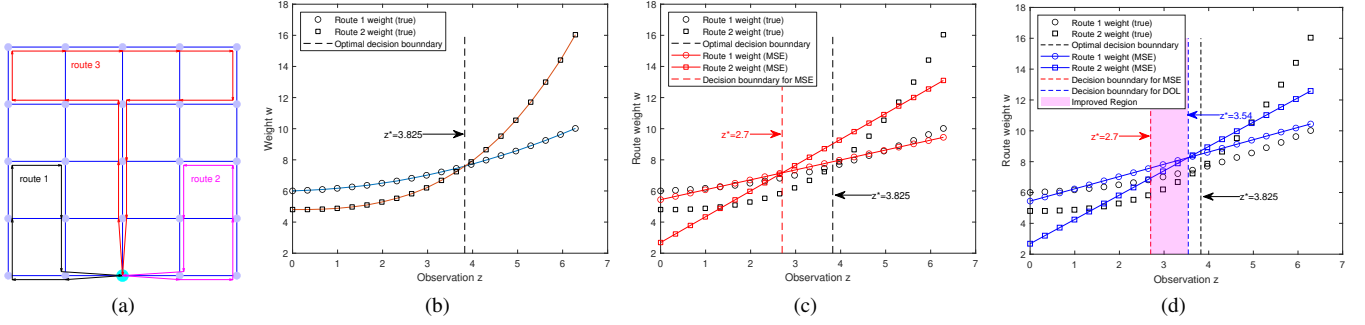


Fig. 4. A case study with three candidate routes and two UGVs. (a) Application scenario. (b) Ground truth data and the optimal decision boundary. (c) Learned linear models using MSE loss. (d) Learned linear models using DOL framework.

where $\hat{w}_i = g(z_i, \theta)$.

Then, the remaining problem is how to compute $\nabla_{\hat{w}_i} \ln p(\hat{\mathcal{S}}_j, \hat{w}_i)$ for a given sample $\hat{\mathcal{S}}_j = (s_1, \dots, s_{|\hat{\mathcal{S}}_j|})$ returned by SG. It should be noticed that $\nabla_{\hat{w}_i} \ln p(\hat{\mathcal{S}}_j, \hat{w}_i) = \nabla_{\hat{w}_i} \ln \prod_{k=1}^{|\hat{\mathcal{S}}_j|} p(s_k, \hat{w}_i) = \sum_{k=1}^{|\hat{\mathcal{S}}_j|} \frac{1}{p(s_k, \hat{w}_i)} \nabla_{\hat{w}_i} p(s_k, \hat{w}_i)$, where $p(s_k, \hat{w}_i)$ can be obtained when we run the SG algorithm. Therefore, we just need to compute $\nabla_{\hat{w}_i} p(s_k, \hat{w}_i)$. Let $p_k(\hat{w}_i)$ be the probability returned by Eq. (8) at the step k corresponding to the sample $\hat{\mathcal{S}}_j$. By using the chain rule,

$$\nabla_{\hat{w}_i} p_k(\hat{w}_i) = \nabla_{m_k} p_k(m_k) \cdot \nabla_{\hat{w}_i} m_k(\hat{w}_i), \quad (14)$$

the row in $\nabla_{\hat{w}_i} p_k(\hat{w}_i)$ corresponding to s_k will give $\nabla_{\hat{w}_i} p(s_k, \hat{w}_i)$. The first term on the r.h.s. of Eq. (14) can be computed using auto-differentiation tools [20] (the objective in (8) is strictly concave) and the second term can be computed by differentiating the parameterized submodular objective.

We can then use the above result to compute the gradient of a batch and update the parameters θ using the stochastic gradient descent method as shown in Algorithm 2.

Algorithm 2: Stochastic Batch Gradient Descent for Problem 1

Input :

- Training data set
- Batch size M and learning rate α

Output: Optimized predictive model g_θ

```

1 while not converge do
2   Select  $M$  training samples randomly
3   for  $i = 1, \dots, M$  do
4      $\hat{w}_i \leftarrow g_{\theta_t}(z_i)$  // predict  $\hat{w}_i$  using  $y_i$ 
5     compute  $\frac{\partial \ell_i}{\partial \theta_t}$ 
6   end
7    $\frac{\partial \ell}{\partial \theta_t} \leftarrow \frac{1}{M} \sum_{i=1}^M \frac{\partial \ell_i}{\partial \theta_t}$ 
8    $\theta_{t+1} \leftarrow \theta_t - \alpha \cdot \frac{\partial \ell}{\partial \theta_t}$ 
9 end
10 return  $g_\theta$ 

```

VI. EXPERIMENTS

We evaluate the performance of the proposed framework in mobile charging station routing problems using synthetic

data. We start with a simple example to build intuitions for the proposed framework in case study I. Then, we will explain the more general setup and show the simulation results in case study II.

A. Case Study I

Let us consider a simple case with three candidate routes and two UGVs as shown in Fig. 4. The three routes (red, black, and magenta curves in Fig. 4a) have no overlaps and the total number of UAVs recharged will be the sum of the number of UAVs recharged in each selected route. Suppose that route 3 (red) has to be included. Then, the problem is to choose one from route 1 (black) and route 2 (magenta). Each route is associated with a weight, which represents the average number of UAVs that will be recharged if the UGV chooses this route, and the goal is to choose the route with a higher weight. We cannot directly know the weights w_1, w_2 at the decision-making time. Instead, we have one scalar observation z (e.g., the orientation of the wind) associated with w_1, w_2 . The training data is given in the form (z_i, w_1^i, w_2^i) and we want to find the mapping from z to the weights of routes. Suppose we want to find a linear model to describe the relationship between observation z and the weights. Fig. 4b shows the training data and the optimal decision boundary (dashed vertical line $z^* = 3.825$, i.e., on the left of this line, we should choose route 1, and on the right, we should choose route 2). If we use mean square error as the objective, we will get two lines as shown in Fig. 4c. The decision boundary (dashed red line, $z^* = 2.7$, passing through the intersection of two learned lines) is on the left of the optimal boundary, thus not optimal. In the region $2.7 \leq z \leq 3.825$, the learned results will lead us to suboptimal decisions, i.e., the optimal decision is to choose route 1 but we will choose route 2. By contrast, if we consider the downstream optimization, we will get two blue lines as shown in Fig. 4d and the decision boundary (dashed blue line, $z^* = 3.54$, passing through the intersection of two learned lines) is much closer to the optimal boundary, which means that the region of z that will lead us to make suboptimal decisions is greatly reduced.

B. Case Study II

1) Simulation Setup:

Environment Model: The working environment is shown

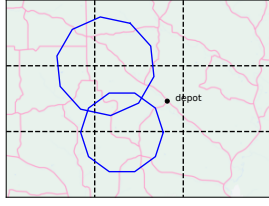


Fig. 5. Working environment for simulation.

in Fig. 5. The magenta lines in the background represent the road network. The task routes of UAVs are shown in blue. There are $n_a = 10$ UAVs and $n_g = 3$ UGVs. The global wind ω is represented as $[a, b, \omega_o]$, where a and b are the shape and scale parameters of Weibull distribution [31], respectively, and ω_o is the wind direction.

UAV Behavior: The route of the UAVs can be of any shape and all routes together can be represented as a top-down-view image as the context input. In this case study, we simplify the representation of the UAV routes. We consider the case that the task route is defined as a sequence of ordered locations uniformly sampled from a circle whose center is $[C_x, C_y]$ and radius is r . Using this geometric information, each route can be represented as a vector C_x, C_y, r . As for the recharging strategy, we use a simple strategy in the simulation: whenever the state of charge drops below 30%, fly to the nearest recharging location waiting for the UGVs. We use the same energy model as that in [29] and details can be found in Appendix.

UGV Routes: After discretizing the road into a connected graph, we generate the candidate routes for UGVs in such a way: we first randomly remove some of the nodes (excluding the depot node) and make sure the left graph is connected. Then, we generate an equivalent complete graph for the left graph and solve a Traveling Salesman Problem to get a route. We generate 15 routes in total for UGVs.

Context Input z and mapping $g_\theta(z)$: As shown in Fig. 1, each z consists of two components: the task routes of all UAVs and the wind field vector $[a, b, \omega_o]$ of the working area. Since the route of the UAV can be parameterized by a circle (C_x, C_y, r) , z can be represented as $[C_x^1, C_y^1, r^1, C_x^2, C_y^2, r^2, \dots, C_x^{n_a}, C_y^{n_a}, r^{n_a}, a, b, \omega_o]$. $g_\theta(z)$ is instantiated using neural networks with one hidden layer (of size 64) with ReLU activation function.

Regularization Function We choose the entropy function for experiments. Specifically, when $\Omega_k(\mathbf{p}) = \epsilon \sum_{i=1}^{n_k} p(u_i) \ln p(u_i)$, where $p(u_i)$ is the i -th entry of $\mathbf{p} \in [0, 1]^{n_k}$ and $\epsilon > 0$ is an arbitrary constant, δ can be set to $\epsilon \ln n_k$. It should be noted that this hyperparameter ϵ controls the value of δ .

Basis Function: For the road graph $G = (V, E)$, we use graph partition algorithms to generate nine sets of nodes, i.e., $\{W_1, \dots, W_9\}$. For each partition $W_i \subset V$, we define three basis functions as in Eq. (6) for decay parameters $\gamma \in \{0.001, 0.5, 1\}$.

2) Generate Training Data:

Raw Data: Based on the UAV UGV behavior models, we

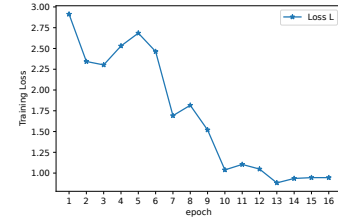


Fig. 6. Per epoch loss curve of DOL.

TABLE I
TEST RESULTS FOR LEARNED MODELS.

Avg # of UAV recharged	DOL	two-stage	random
$n_a = 6, n_g = 3$	5.3 ± 0.5	4.6 ± 0.4	2.1 ± 1.4
$n_a = 10, n_g = 3$	9.2 ± 0.7	8.5 ± 0.6	4.5 ± 1.3
$n_a = 15, n_g = 4$	14.1 ± 0.8	13.2 ± 0.7	7.5 ± 1.6

build a simulator for the routing problems. Given simulation parameters (e.g., UAV routes, and wind conditions), it will simulate UAVs' execution of persistent tasks. If we provide several selected routes to the simulator, it will return the number of UAVs recharged if UGV follows these routes. Based on this simulator, for each context observation z , we test multiple possible route selections and obtain a set of the actual number of UAVs that UGV recharged. We will use this raw data to obtain the training data for the decision-oriented learning framework.

To train the decision-oriented framework proposed in Sec. III, we need the i -th data point to be in the form (z_i, w_i) , where z_i denotes the context input and w_i is the corresponding parameter vector of the objective function. However, w_i is not directly available and we need to do some pre-processing of the raw data. Specifically, for each z , we have a set of values for different selections, i.e., $\mathcal{F} = \{f(\mathcal{S}_1), \dots, f(\mathcal{S}_{|\mathcal{F}|})\}$. We find the corresponding w by solving the following regularized least square optimization problem [30]:

$$\min_{w \geq 0} \sum_{i=1}^{|\mathcal{F}|} \|f(\mathcal{S}_i, w) - f(\mathcal{S}_i)\|_2^2 + \xi \|w\|_2^2, \quad (15)$$

where ξ is a user-specified regularization parameter.

We use the Gurobi optimization solver for solving the problem (8) and use Pytorch to implement the neural network. All experiments are conducted using Python 3.9 on a PC with the i9-8950HK processor and 32GB memory.

3) Results:

Fig. 6 shows the learning curves over epochs. In each epoch, we compute the gradient by sampling a batch size of 40 in each iteration. We can see that as the training epoch increases, the loss will gradually decrease to a steady value. It should be noticed that the loss here represents the solution quality gap between the solution obtained using ground truth parameters and the solution obtained using predicted parameters as defined in Problem 1. Therefore, such a decrease

suggests that the decision quality is improving.

After training, we test the performance of the learned models using the simulator. We generate a set of context observations $\{z_i\}_{\text{test}}$ and compute the corresponding predicted weights $\{\hat{w}_i\}_{\text{test}}$. Then, we use $\{\hat{w}_i\}_{\text{test}}$ to select routes and feed the route to the simulator to obtain the actual number of UAVs recharged. The result is shown in Table VI-B.2. We compare three approaches: DOL (our), two-stage (classic supervise learning with MSE loss), and random (select routes randomly without any learning). As shown in Table VI-B.2, our approach on average can result in better route selection and recharge more UAVs.

VII. CONCLUSION

We propose a decision-oriented learning framework for mobile charging routing problems. We first show how to formulate the learning problem in the context of mobile charging routing. Then, we show how to make submodular maximization a differentiable layer by using stochastic smoothing techniques. The proposed framework and formulation are validated through several case studies.

Our work will be extended in two directions in future work. The first direction is to consider the case that we need to predict not a value but a distribution and the downstream task is defined over such distribution (e.g., risk-sensitive metric). The second direction is to generalize the smoothed greedy algorithm to a broader range of approximately submodular objectives.

REFERENCES

- [1] Y. Kantaros, B. Schlotfeldt, N. Atanasov, and G. J. Pappas, "Asymptotically optimal planning for non-myopic multi-robot information gathering," in *Robotics: Science and Systems*, 2019, pp. 22–26.
- [2] K.-C. Ma, Z. Ma, L. Liu, and G. S. Sukhatme, "Multi-robot informative and adaptive planning for persistent environmental monitoring," in *Distributed Autonomous Robotic Systems: The 13th International Symposium*. Springer, 2018, pp. 285–298.
- [3] X. Xu, G. Shi, P. Tokekar, and Y. Diaz-Mercado, "Interactive multi-robot aerial cinematography through hemispherical manifold coverage," in *2022 IEEE/RSJ International Conference on Intelligent Robots and Systems (IROS)*. IEEE, 2022, pp. 11 528–11 534.
- [4] L. E. Parker, "Decision making as optimization in multi-robot teams," in *International Conference on Distributed Computing and Internet Technology*. Springer, 2012, pp. 35–49.
- [5] A. Krause, A. Singh, and C. Guestrin, "Near-optimal sensor placements in gaussian processes: Theory, efficient algorithms and empirical studies," *Journal of Machine Learning Research*, vol. 9, no. 2, 2008.
- [6] L. Zhou, V. Tzoumas, G. J. Pappas, and P. Tokekar, "Resilient active target tracking with multiple robots," *IEEE Robotics and Automation Letters*, vol. 4, no. 1, pp. 129–136, 2018.
- [7] K.-S. Tseng and B. Mettler, "Near-optimal probabilistic search via submodularity and sparse regression," *Autonomous Robots*, vol. 41, no. 1, pp. 205–229, 2017.
- [8] G. L. Nemhauser, L. A. Wolsey, and M. L. Fisher, "An analysis of approximations for maximizing submodular set functions—I," *Mathematical programming*, vol. 14, pp. 265–294, 1978.
- [9] D. Mitchell, N. Chakraborty, K. Sycara, and N. Michael, "Multi-robot persistent coverage with stochastic task costs," in *2015 IEEE/RSJ International Conference on Intelligent Robots and Systems (IROS)*. IEEE, 2015, pp. 3401–3406.
- [10] J. Derenick, N. Michael, and V. Kumar, "Energy-aware coverage control with docking for robot teams," in *2011 IEEE/RSJ International Conference on Intelligent Robots and Systems*. IEEE, 2011, pp. 3667–3672.
- [11] L. Liu and N. Michael, "Energy-aware aerial vehicle deployment via bipartite graph matching," in *2014 International Conference on Unmanned Aircraft Systems (ICUAS)*. IEEE, 2014, pp. 189–194.
- [12] K. Yu, J. M. O’Kane, and P. Tokekar, "Coverage of an environment using energy-constrained unmanned aerial vehicles," in *2019 international conference on robotics and automation (ICRA)*. IEEE, 2019, pp. 3259–3265.
- [13] G. Shi, N. Karapetyan, A. B. Asghar, J.-P. Reddinger, J. Dotterweich, J. Humann, and P. Tokekar, "Risk-aware uav-ugv rendezvous with chance-constrained markov decision process," *The 61th IEEE Conference on Decision and Control (CDC)*, 2022.
- [14] A. B. Asghar, G. Shi, N. Karapetyan, J. Humann, J.-P. Reddinger, J. Dotterweich, and P. Tokekar, "Risk-aware resource allocation for multiple uavs-ugvs recharging rendezvous," *Proceedings of the IEEE International Conference on Robotics and Automation (ICRA)*, 2023.
- [15] A. N. Elmachtoub and P. Grigas, "Smart "predict, then optimize"," *Management Science*, vol. 68, no. 1, pp. 9–26, 2022.
- [16] B. Wilder, B. Dilkina, and M. Tambe, "Melding the data-decisions pipeline: Decision-focused learning for combinatorial optimization," in *Proceedings of the AAAI Conference on Artificial Intelligence*, vol. 33, no. 01, 2019, pp. 1658–1665.
- [17] J. Mandi, P. J. Stuckey, T. Guns *et al.*, "Smart predict-and-optimize for hard combinatorial optimization problems," in *Proceedings of the AAAI Conference on Artificial Intelligence*, vol. 34, no. 02, 2020, pp. 1603–1610.
- [18] N. Wilde, A. Sadeghi, and S. L. Smith, "Learning submodular objectives for team environmental monitoring," *IEEE Robotics and Automation Letters*, vol. 7, no. 2, pp. 960–967, 2021.
- [19] B. Amos and J. Z. Kolter, "Optnet: Differentiable optimization as a layer in neural networks," in *International Conference on Machine Learning*. PMLR, 2017, pp. 136–145.
- [20] A. Agrawal, B. Amos, S. Barratt, S. Boyd, S. Diamond, and J. Z. Kolter, "Differentiable convex optimization layers," *Advances in neural information processing systems*, vol. 32, 2019.
- [21] S. Muntwiler, K. P. Wabersich, and M. N. Zeilinger, "Learning-based moving horizon estimation through differentiable convex optimization layers," in *Learning for Dynamics and Control Conference*. PMLR, 2022, pp. 153–165.
- [22] B. Amos, I. Jimenez, J. Sacks, B. Boots, and J. Z. Kolter, "Differentiable mpc for end-to-end planning and control," *Advances in neural information processing systems*, vol. 31, 2018.
- [23] S. Chen, K. Saulnier, N. Atanasov, D. D. Lee, V. Kumar, G. J. Pappas, and M. Morari, "Approximating explicit model predictive control using constrained neural networks," in *2018 Annual American conference (ACC)*. IEEE, 2018, pp. 1520–1527.
- [24] M. Bhardwaj, B. Boots, and M. Mukadam, "Differentiable gaussian process motion planning," in *2020 IEEE international conference on robotics and automation (ICRA)*. IEEE, 2020, pp. 10 598–10 604.
- [25] A. Ferber, B. Wilder, B. Dilkina, and M. Tambe, "Mipaal: Mixed integer program as a layer," in *Proceedings of the AAAI Conference on Artificial Intelligence*, vol. 34, no. 02, 2020, pp. 1504–1511.
- [26] M. V. Pogačić, A. Paulus, V. Musil, G. Martius, and M. Rolinek, "Differentiation of blackbox combinatorial solvers," in *International Conference on Learning Representations*, 2019.
- [27] J. Djolonga and A. Krause, "Differentiable learning of submodular models," *Advances in Neural Information Processing Systems*, vol. 30, 2017.
- [28] S. Sakaue, "Differentiable greedy algorithm for monotone submodular maximization: Guarantees, gradient estimators, and applications," in *International Conference on Artificial Intelligence and Statistics*. PMLR, 2021, pp. 28–36.
- [29] F. B. Sorbelli, F. Corò, S. K. Das, and C. M. Pinotti, "Energy-constrained delivery of goods with drones under varying wind conditions," *IEEE Transactions on Intelligent Transportation Systems*, vol. 22, no. 9, pp. 6048–6060, 2020.
- [30] S. Tschitschek, R. K. Iyer, H. Wei, and J. A. Bilmes, "Learning mixtures of submodular functions for image collection summarization," *Advances in neural information processing systems*, vol. 27, 2014.
- [31] J. Seguro and T. Lambert, "Modern estimation of the parameters of the weibull wind speed distribution for wind energy analysis," *Journal of wind engineering and industrial aerodynamics*, vol. 85, no. 1, pp. 75–84, 2000.

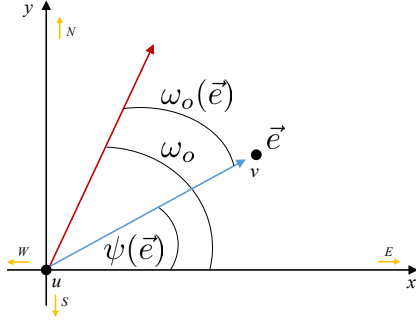


Fig. 7. Relative wind directions.

VIII. APPENDIX

A. UAV Energy Consumption Model

Wind Model: Let the global wind $\omega = (\omega_s, \omega_o)$ be the wind in the working area \mathcal{E} , where ω_s and ω_o are wind speed and direction, respectively and ω_s is a random variable with Weibull distribution [31]. The PDF of ω_s is given as

$$p(\omega_s; a, b) = \begin{cases} \frac{a}{b} \left(\frac{\omega_s}{a}\right)^{b-1} e^{-\left(\frac{\omega_s}{a}\right)^b} & \text{if } \omega_s \geq 0 \\ 0 & \text{otherwise,} \end{cases} \quad (16)$$

where $a > 0$ is the shape parameter and $b > 0$ is the scale parameter.

When the UAV is traversing an edge $\vec{e} = (u, v)$, we build a Cartesian coordinate system with origin in u as shown in Fig. 7 and define the *relative wind direction* as $\omega_o(\vec{e}) = \omega_o - \psi(\vec{e})$, where

$$\psi(\vec{e}) = \begin{cases} \arctan\left(\frac{y_v}{x_v}\right) \bmod 360^\circ & \text{if } x_v > 0 \\ 180^\circ + \arctan\left(\frac{y_v}{x_v}\right) & \text{if } x_v < 0 \end{cases} \quad (17)$$

is the direction of the edge \vec{e} .

Energy Model: The total required thrust when the UAV is flying is

$$T = Wg + F_D, \quad (18)$$

where W is the weight of the UAV; g is the gravitational constant; and $F_D = \frac{1}{2}\rho s_a(\vec{e})^2 C_D A$ is the total drag force with ρ being the air density, A being the surface area, C_D being the drag coefficient. $s_a(\vec{e})$ depends on the global wind speed and the relative wind direction and can be computed as

$$s_a(\vec{e}) = \sqrt{s_N^2 + s_E^2}, \quad (19)$$

where $s_N = s_d - \omega_s \cos \omega_o(\vec{e})$ (s_d is the drone speed) and $s_E = -\omega_s \sin \omega_o(\vec{e})$.

The power consumption for a steady flight under thrust T can be computed as

$$P = T(s_d \sin \alpha + s_i), \quad (20)$$

where $\alpha = \arctan\left(\frac{F_D}{Wg}\right)$ is the pitch angle; s_i is the induced velocity required for a given thrust T and can be computed as

$$s_i = \frac{s_h^2}{\sqrt{(s_d \cos \alpha)^2 + (s_d \sin(\alpha) + s_i)^2}}, \quad (21)$$

where $s_h = \sqrt{\frac{T}{2\rho A}}$ is the induced velocity at hover.

Hence, for a global wind $\omega = (\omega_s, \omega_o)$, the energy efficiency (i.e., energy consumption per unit distance) can be computed as

$$\mu_\omega(\vec{e}) = \frac{P}{s_d}. \quad (22)$$

Therefore, the total energy consumption for traversing and edge \vec{e} with the length $\lambda(\vec{e})$ is

$$E_\omega(\vec{e}) = \mu_\omega(\vec{e})\lambda(\vec{e}). \quad (23)$$